

## NANODECORATION OF SINGLE CRYSTALS OF 5,11,17,23-TETRA-*TERT*-BUTYL-25,27-BIS(CYANOMETHOXY)-26,28-DIHYDROXYCALIX[4]AREN

S. MORIS<sup>1\*</sup>, N. SILVA<sup>2,5</sup>, C. SAITZ<sup>3</sup>, P. JARA<sup>2</sup>, B. CHORNIK<sup>4</sup>

<sup>1</sup>Vicerrectoría de Investigación y postgrado, Universidad Católica del Maule, Avenida San Miguel, Chile.

<sup>2</sup>Facultad de Ciencias, Departamento de Química, Universidad de Chile, Las Palmeras 3425, Santiago, 7800003 Chile.

<sup>3</sup>Departamento de Química Orgánica y Fisicoquímica, Facultad de Ciencias Químicas y Farmacéuticas, Universidad de Chile, Sergio Livingstone 1007, Santiago 8380492, Chile.

<sup>4</sup>Departamento de Física, Universidad de Chile, Beauchef 850, Santiago 8370448, Chile.

<sup>5</sup>Departamento de Química de Materiales, Universidad de Santiago de Chile, Av. Libertador Bernardo O'Higgins 3363, Santiago 9170022, Chile

### ABSTRACT

Single crystals of 1,3-bis(cyanomethoxy)calix[4]arene (**1**) were grown from Chloroform/Methanol mixture and these were nanodecorated with colloidal gold nanoparticles (AuNPs). The single crystals were then characterized by single-crystal X-ray diffraction (XRD) and Scanning Electronic Microscopy (SEM). The nanodecorated crystals were characterized by UV-Visible Absorption Spectroscopy, Transmission Electronic Microscopy (TEM) and X-ray Photoelectron Spectroscopy (XPS). In this work, it is shown that the stabilization of the nanoparticles occurs through of the interactions of these with the nitrile group, maintaining their shape and size.

**Keywords:** Single crystals, 1,3-bis(cyanomethoxy)calix[4]arene, nanodecorated, Gold Nanoparticles.

### 1. INTRODUCTION

Calixarenes are synthetic cyclooligomers formed via a phenol-formaldehyde condensation<sup>1</sup>. Calix[n]arenes adopt a basket-shaped conformation in their solid state, with a ring size which depends on the base used<sup>2</sup>. These macrocycles have been the subject of a variety of studies because of their interesting and technologically useful properties<sup>3-4</sup>.

Calixarenes have interesting applications as host molecules because of their preformed cavities<sup>5</sup>. Carrying out different chemical modifications in the groups at the upper and/or lower rim, it is possible to prepare a series of derivatives with differing selectivities for various guest ions and molecules<sup>6-7</sup>. This is due to the interactions that occur between the hydrophilic areas of calix[n]arenes (lower rim) and different species. These interactions are primarily hydrogen bonds<sup>8</sup>. Moreover, these compounds may host different molecules or ions within the hydrophobic cavity due to the interactions generated by the aromatic fraction<sup>9</sup>. Different types of guests, including neutral molecules<sup>10,11</sup> such as acetonitrile<sup>12</sup>, and various ions<sup>13,14</sup>, have been reported.

The 5,11,17,23-Tetra-*tert*-butyl-25,27-bis(cyanomethoxy)-26,28-dihydroxycalix[4] arene (**1**) (dicyanocalix[4]arene) corresponds to *p*-*tert*-butylcalix[4]arene having a nitrile group 1,3-distal in its lower rim part<sup>2</sup>. This calixarene derivative can be obtained as a single crystal<sup>15</sup> because of their organization forming a supramolecular assembly due to different interactions, such as hydrogen bonds and CH-π interactions with dicyanocalix[4]arenes neighbors<sup>16</sup>. This supramolecular arrangement allows the attachment of gold nanoparticles (AuNPs) on the surface of a single crystal, maintaining their shape and size.

As well as in cyclodextrin<sup>17</sup> and other supramolecular macrocycles<sup>18</sup>, nanodecoration of these compounds would allow the manufacturing of nanoscale devices with potential applications as sensors, switches and new materials having tunable properties<sup>19,20</sup>.

In this work, we present the supramolecular analysis of dicyanocalix [4] arene, and the confirmation of the stabilization of nanoparticles by functional -CN group responsible for the formation of the crystal-nanodecoration.

### 2. MATERIAL AND METHODS

#### 2.1. Reagents and instruments

All the reagents used were of analytical reagent grade. *p*-*tert*-butylcalix[4] arene and gold chloride trihydrate (HAuCl<sub>4</sub>.3H<sub>2</sub>O) (Aldrich, >99%), Na<sub>3</sub>C<sub>6</sub>H<sub>5</sub>O<sub>7</sub> (Sigma-Aldrich), and nanopure water (Merck, Darmstadt, Germany). All Solvents employed for synthesis were commercially available and used as received without further purification. TEM was performed using a Zeiss model EM-109 microscope (Jena, Germany) operating at 80 kV (IBEC, Barcelona, Spain). SEM images were obtained using a high-resolution NOVA NanoSEM 230 instrument (FEI Company) equipped with an energy-dispersive detector.

Single-Crystal XRD data were collected at room temperature using a Bruker Kappa CCD diffractometer with graphite-monochromatized MoKα radiation ( $\lambda=0.71073 \text{ \AA}$ ). A Shimadzu UV-3101PC spectrophotometer (Shimadzu, Kyoto, Japan) was used. Spectra were recorded between 400 and 700 nm for colloidal nanoparticles. The diffuse reflectance results were converted into absorbance units using Kubelka-Munk conversion for de solid-state compounds.

XPS spectra were recorded using a photoelectron spectrometer model 1257 (Perkin Elmer, Physical Electronic Division, Eden Prairie, MN, USA), fitted with an ultra-high-vacuum main chamber, a hemispherical electron analyzer, and an X-ray source that provided unfiltered Al Kα radiation. Energy calibration was accomplished by assigning a binding energy of 284.8 eV to the C 1s peak of adventitious carbon<sup>21</sup>.

#### 2.2 Synthesis of 5,11,17,23-Tetra-*tert*-butyl-25,27-bis(cyanomethoxy)-26,28-dihydroxycalix [4] arene (**1**)

This compound is obtained as described by Zhang<sup>2</sup>. Single-crystals were obtained from a solution of (**1**) (0.6 mmol) in boiling chloroform (0.5 mL) with hot methanol added dropwise (1 mL). This solution was left for one week, at which point laminar crystals were observed and dried<sup>9</sup>.

Part of the crystals obtained was selected with a stereoscopic lens to be characterized by single-crystal x-ray diffraction, obtaining their crystalline structures, and then the crystals were characterized by scanning electron microscopy in order to know their morphology.

#### 2.3 Synthesis of gold nanoparticles

The gold nanoparticles was synthesized in accordance with the Turkevich method<sup>22</sup>. 100 mL of an aqueous HAuCl<sub>4</sub> solution (1 mM) was brought to boil in a 250-mL round-bottomed flask, equipped with a condenser and under vigorous stirring. As quickly as possible, 10 mL of Na<sub>3</sub>C<sub>6</sub>H<sub>5</sub>O<sub>7</sub> solution (38.8 mM) was added under continuous stirring. The solution was heated for an additional 30 min and then allowed to cool to room temperature. Then, the solution was filtered through a 0.45-μm cellulose acetate membrane filter<sup>23</sup>. This synthesis allows obtaining gold nanoparticles (AuNPs) of controlled diameter less than 15 nm<sup>24</sup>.

Nanoparticles were characterized by UV-Visible Absorption Spectroscopy and TEM.

#### 2.4 Nanodecoration of (**1**)

Crystals of (**1**) (0.1 g) was immersed in a solution of AuNPs (500 μL) at room temperature (at pH 7) and was subsequently washed with a 38.8 mM (500 μL) citrate solution to remove AuNPs that had not adhered. Finally, the sample of AuNPs that had adhered to the crystals of (**1**) was dried under vacuum<sup>24</sup>.

The nanodecorated compound was characterized by diffuse reflectance

spectrophotometry UV-Vis, transmission electron microscopy (TEM), scanning electron microscopy (SEM) and X-ray photoemission spectroscopy (XPS).

### 2.5 Crystallography

The H atoms of O2, O4, C45 and C46 were found in electron density maps and were refined freely. The remaining H atoms are placed geometrically with C-H = 0.97 to 0.93 Å. Shift factors were taken as Uiso (H) = 1.2Ueq (C) and Uiso (H) = 1.5Ueq (C). The crystallographic data is summarized in Table 1.

Data collection: Bruker SMART (BRUKER 1996, Madison, WI, USA); cell refinement: Bruker SAINTPLUS V6.02 (BRUKER 1997); data reduction: Bruker SHELXTL V6.10 (BRUKER 2000); program used to solve the structure: SHELXS97 (Sheldrick, 1990, Madison, WI, USA); program used to refine the structure: SHELXL97 (Sheldrick, 1997, Stuttgart, Germany)<sup>25,26</sup>. Molecular graphics: DIAMOND (Brandenburg, 1999, Bonn, Germany); software used to prepare the material for publication: PLATON (Spek, 2003, Utrecht, The Netherlands)<sup>27,28</sup>.

**Table 1.** Crystallographic data of dicyanocalix [4] arene (**1**).

<b>Empirical Formula</b>	C <sub>48</sub> H <sub>58</sub> N <sub>2</sub> O <sub>4</sub>
<b>Crystal size (mm<sup>3</sup>)</b>	0.50 x 0.20 x 0.09
<b>Crystal system</b>	Triclinic
<b>Space group, Z</b>	P-1, 2
<b>Unit Cell Dimensions</b>	a=10.445(2), b=13.187(3), c=16.759(3) Å α= 84.96(3) β=79.65(3) γ= 86.83(3)
<b>Volume (Å)</b>	2260.2(8)
<b>Absorption coefficient</b>	0.067
<b>F (000)</b>	784
<b>θ range for data collection</b>	3.6, 25.0
<b>Range of h, k, l</b>	-12/12, -15/15, -19/19
<b>R<sub>int</sub>, R<sub>o</sub></b>	0.0865, 0.0772
<b>Reflections collected</b>	27070
<b>Independent Reflections</b>	4071
<b>Parameters</b>	525
<b>R and wR2 [I&gt;2σ (I)]</b>	0.0801, 0.1557
<b>Goodness-of-fit on F<sup>2</sup> (Goof=S)</b>	1.169
<b>Residual electron densities (e Å<sup>-3</sup>)</b>	-0.29 a 0.51
<b>Temperature</b>	293 K

### 3. RESULTS AND DISCUSSION

#### 3.1. Crystal structure

The crystal was solved newly considering what is proposed by Collins<sup>15</sup>, and analyzed intermolecular interactions and supramolecular packing of this compound were analyzed as well.

Fig. 1 shows ORTEP plot of the crystal structure of compound (**1**), in which the cone conformation can be observed, this conformation is established due to the intramolecular hydrogen bonds between OH<sup>-</sup> groups in the lower rim of the compound (Fig. 2 S2).

In the crystal packing of the compound, the molecules are linked by hydrogen bonds, weak intermolecular C-H···O(N) contacts and C-H···π interactions (Table 2). The intramolecular hydrogen-bonds that are involved in O2—H2A···O3 and O4—H2A···O1, generate two graph-set descriptor S(8) motifs (Fig. 3, Table 2).

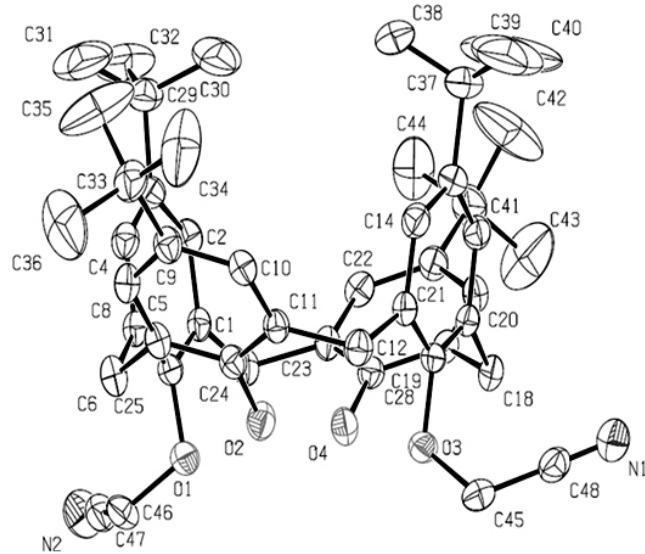
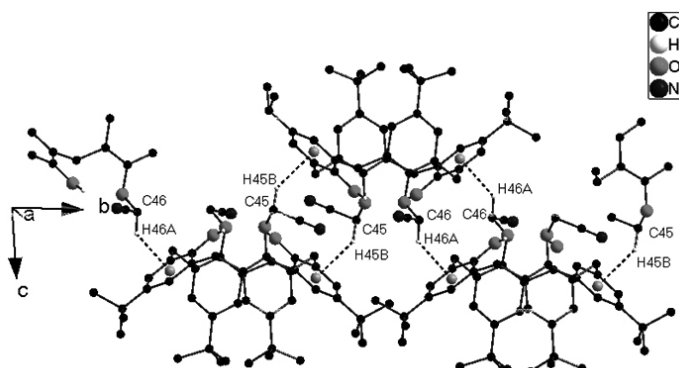


**Fig. 1.** ORTEP plot of the crystal structure of dicyanocalix[4]arene. The hydrogen atoms have been omitted for clarity.

**Table 2.** Intermolecular contacts of dicyanocalix[4]arene.

D-X...A	d(D-X)	d(X...A)	d(D...A)	<(DXA)
O2--H2A ... O3 <sup>i</sup>	0.64(6)	2.32(5)	2.936(4)	163(8)
O4 -- H4A ...O1 <sup>i</sup>	0.78(7)	2.18(7)	2.907(4)	156(6)
C46-H46A...Cg2 <sup>ii</sup>	1.05(5)	2.55(4)	3.393(5)	137(3)
C45H45B...Cg4 <sup>iii</sup>	1.08(3)	2.57(4)	3.519(4)	145(3)

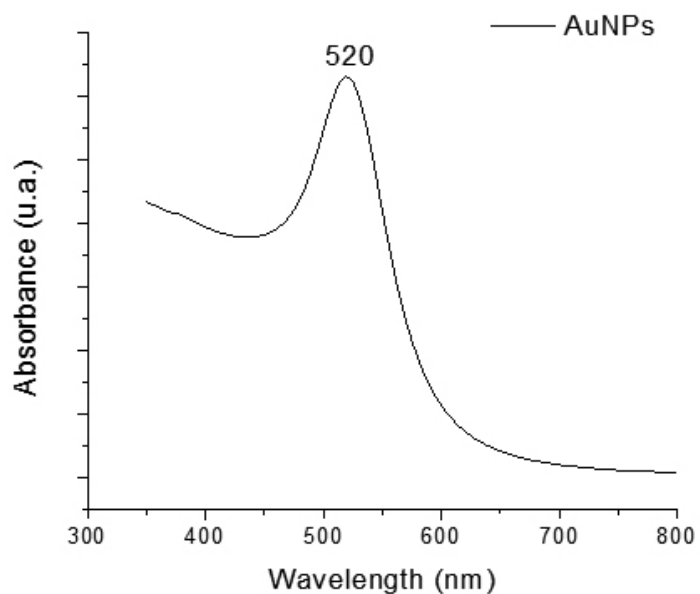
Symmetry Codes: (i) x,y,z, (ii)1-x,2-y,2-z, (iii) 1-x,1y,2z.



**Fig. 3.** Supramolecular array of the dicyanocalix[4]arene formed by CH-π interactions.

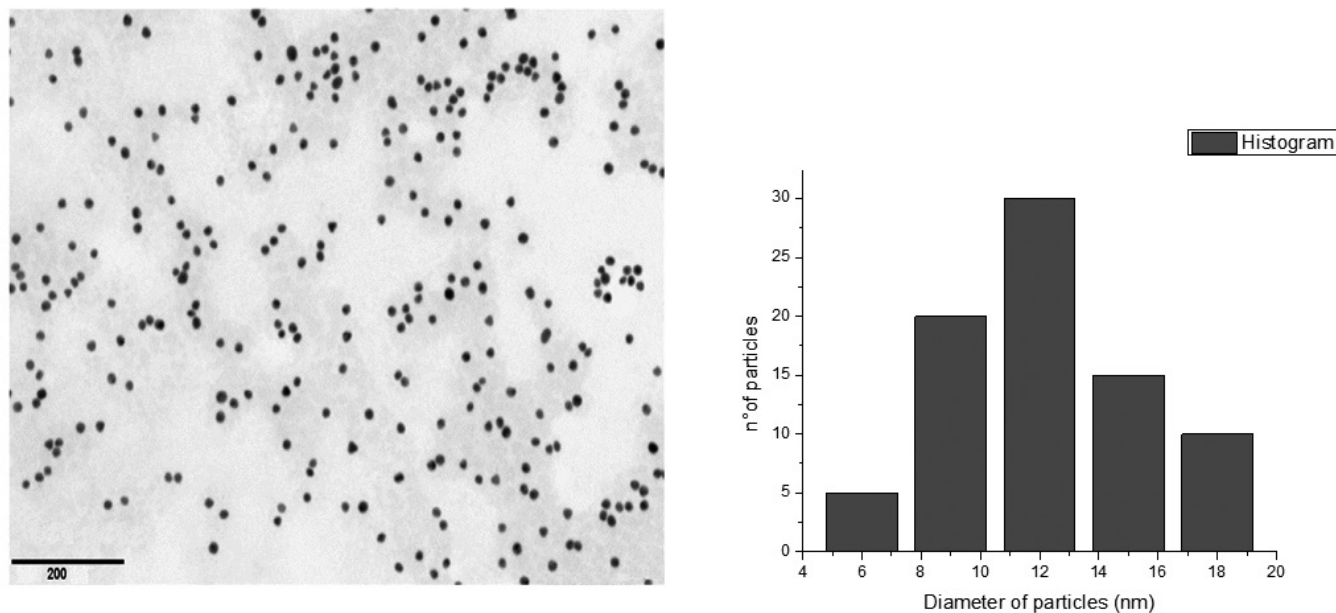
#### 3.2. Nanoparticles and nanodecorated

Gold Nanoparticles were characterized by UV-Visible Absorption Spectroscopy and transmission electronic microscopy (TEM) as shown in fig. 5 and 6.



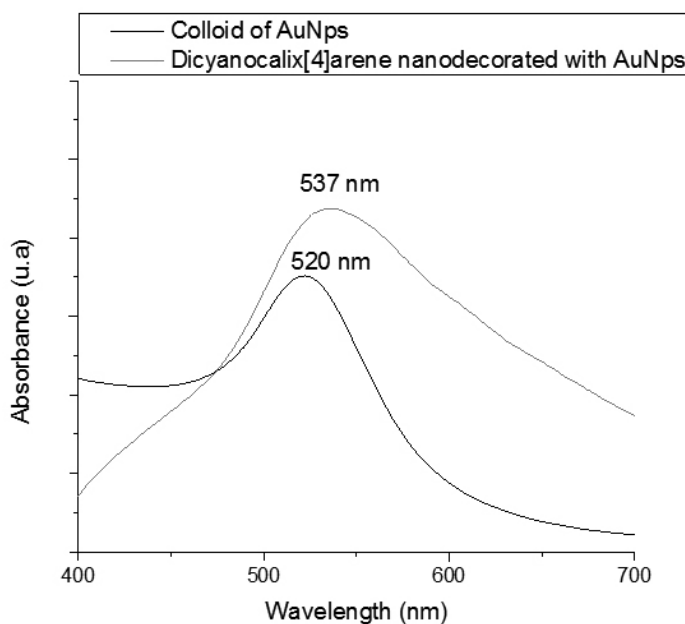
**Fig. 5.** UV-Vis spectra of gold nanoparticles.

Fig. 5 presents the absorption spectra of samples of citrate-stabilized colloidal AuNPs and shows an absorption maximum at 520 nm, characteristic sign of colloidal AuNPs with less than 20 nm diameter and spherical shape<sup>17</sup>. This information is corroborated by TEM as shown in fig. 6.



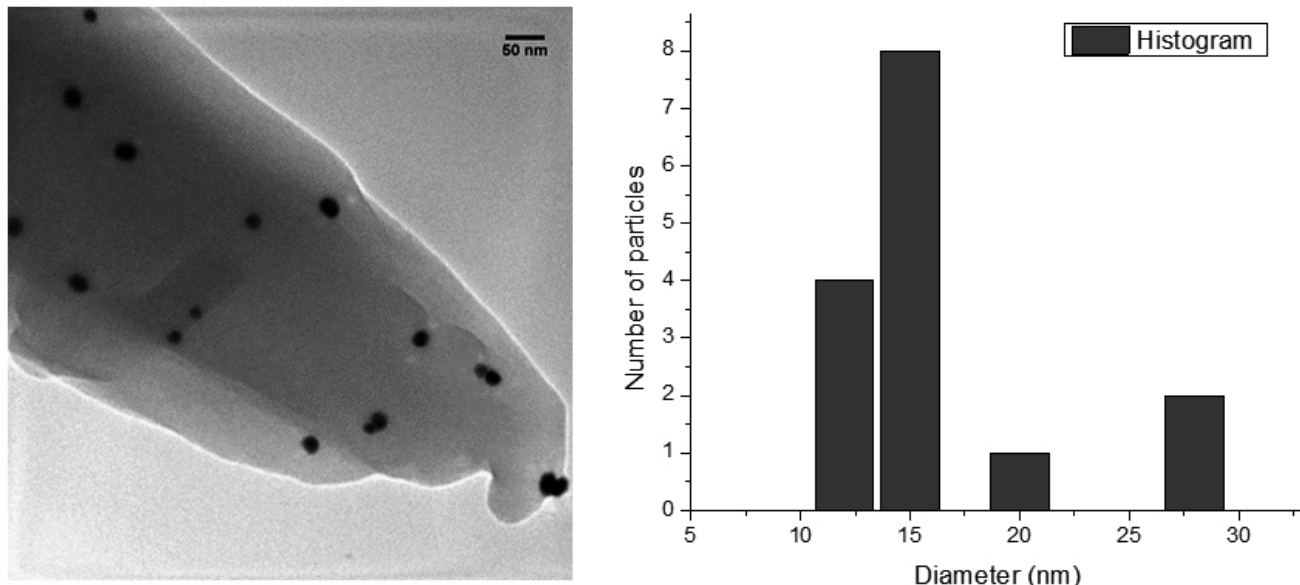
**Fig. 6.** TEM Microscopy of AuNPs with histogram of diameter.

In the fig. 6 are seen spherical gold nanoparticles with low size dispersion, this is demonstrated with the histogram where dominated AuNPs with 12 nm of diameter. The solid dicyanocalix[4]arene nanodecorated was characterized by Diffuse reflectance spectrophotometry, scanning electron microscopy (SEM), and electron transmission microscopy (TEM).



**Fig. 7.** Comparative spectra of gold colloid and dicyanocalix[4]arene nanodecorated.

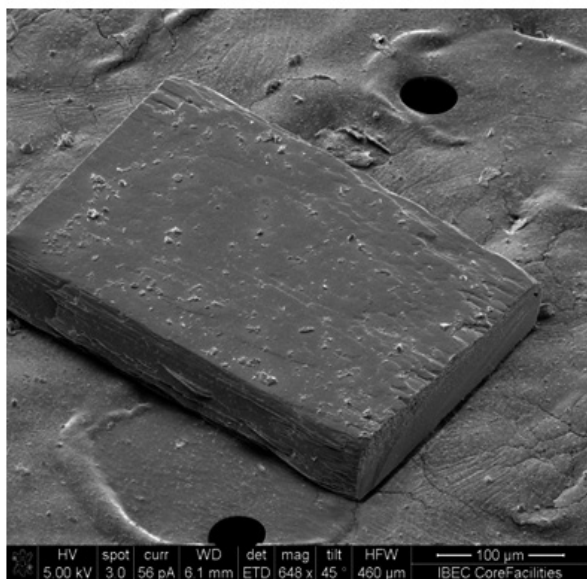
In the fig. 7 for de AuNPs fixed to single crystal of (**1**) a broadening and a bathochromic shift of this plasmon band is observed at 537 nm, due to a change in the dielectric environment provided by the dicyanocalix[4]arene and dipolar coupling between closely neighboring particles<sup>17</sup>. Any change in the shape and size is verified by TEM as shown in fig. 8.



**Fig. 8.** TEM micrographs of dicyanocalix[4]arene nanodecorated.

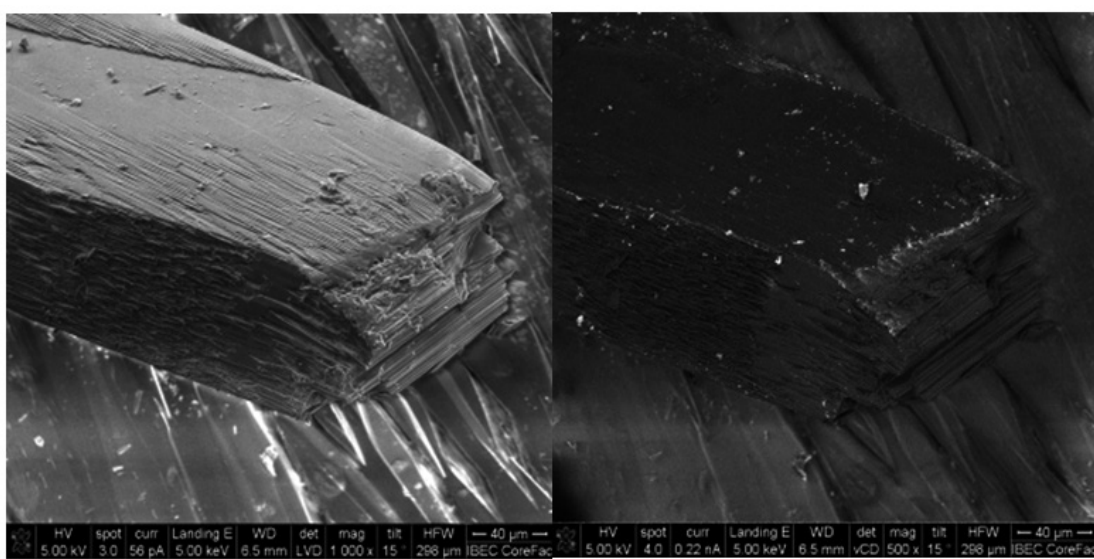
TEM Micrographs in fig.8 show spherical gold nanoparticles between 10-30 nm of diameter on the surface of dicyanocalix[4]arene. This slight increase in size contributes to shift wavelengths greater than the maximum absorption of samples of citrate-stabilized colloidal AuNPs.

SEM micrographs show a single crystal morphology and gold nanoparticles nanodecorates the surface of this crystal.



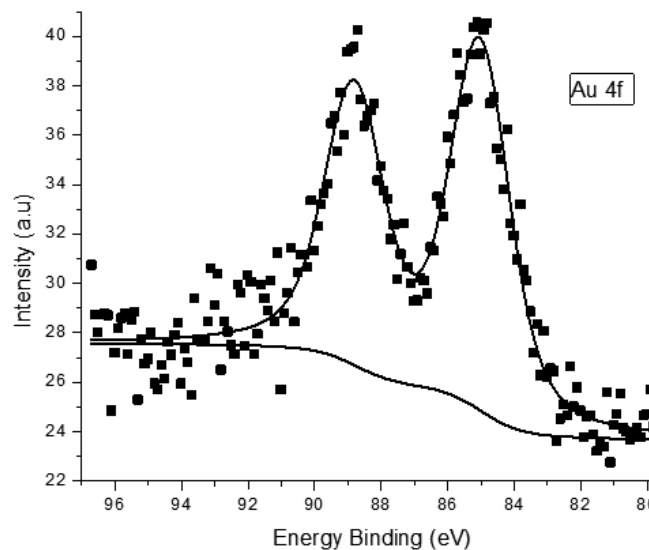
**Fig. 9.** SEM micrograph of a single crystal of dicyanocalix[4]arene.

Fig. 9 shows SEM micrograph of a single crystal like sheet with sharp edges and homogeneous surface.  
The single crystal nanodecorated shows in fig.10.



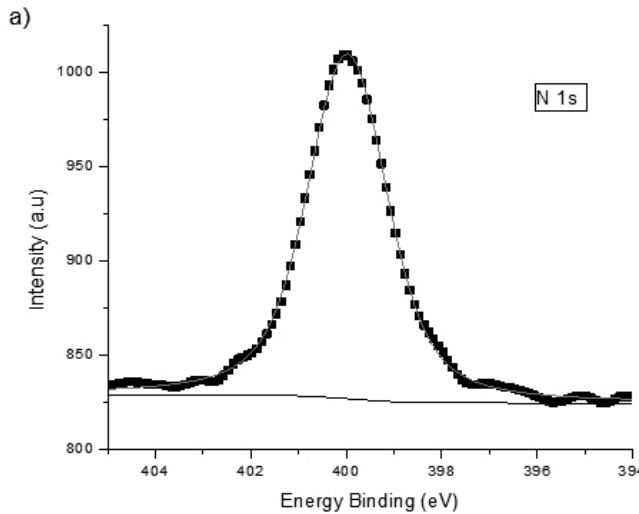
**Fig. 10.** SEM micrographs of dicyanocalix[4]arene nanodecorated, right side LVD detectors and VCD (Backscattering).

Fig.10 shows preferential zones within the surface of the crystals of calixarene (**1**) where AuNps are deposited. The backscattering technique used in the micrographs (right micrograph) allows the identification of the AuNps covered areas and differentiate them from the compound areas that do not interact with the AuNps. By means of this technique it is possible to identify areas where the population of AuNps is denser, as well as zones with absence of AuNps on the surface of the crystal.



**Fig. 11.** Spectrum Xps of the region 4f of gold of AuNPs on the calixarene (I)

Fig. 11 shows an Xps spectrum of the region 4f of gold for calixarene (I). The levels  $\text{Au } 4f_{7/2}$  and  $\text{Au } 4f_{5/2}$  present peaks located at 85.02 and 88.81 eV respectively, higher values compared to the value corresponding to pure gold<sup>29</sup>. The increase in the magnitude of these signals is due to some gold atoms that have been oxidized after the union with calixarene (I)<sup>30</sup>.



**Fig. 12.** XPS spectrum of binding energy for the nitrogen 1s. a) for the pure calixarene (I).

Fig. 12 a) shows the spectrum of the 1s region of N of the calixarene (I). The Xps deconvolution spectrum for the pure compound shows a signal at 399.97 eV which is consistent with that for nitrogen attached to carbon<sup>31</sup>.

The nitrogen 1s of the nanodecorated calixarene (I) is shown in fig. 12 Bb). In the spectrum, a decrease to 399.89 eV in the maximum energy is observed. This could be due to the delivery of electrons from the gold to the nitrogen reducing the oxidation state of the nitrogen. This shift of binding energy of the N1s to a lower level has also been observed in DNA chemisorbed on gold surfaces<sup>32</sup>.

Calixarene crystals as well as inclusion compounds of cyclodextrin have the ability to form nanodecorates, maintaining the shape and size of the gold nanoparticles<sup>24</sup>. However, unlike these, it does not require an inclusion compound, but the chemical modification of a functional group affined to AuNPs, as is the cyano group.

## CONCLUSIONS

Dicyanocalix[4] arene (**1**) has the capability to stabilize gold nanoparticles due to a supramolecular array produced by different intra and intermolecular interactions, such as hydrogen bonds and C-H···π interactions. The supramolecular array shows interaction between the lower rim of a molecule to dicyanocalix[4]arene with the aromatic centroid of another molecule of dicyanocalix[4]arene.

The packing shows a preferential plane where the functional -CN groups are located exposed for nanodecoration. The SEM technique with backscattered electrons allows confirming this preferential zone where nanoparticles are located with a high population density.

Stabilization of AuNPs occurs due to the strong interaction of nitrogen atoms with AuNPs. This is confirmed by the XPS spectroscopy

## ACKNOWLEDGMENTS

The authors wish to thank CONICYT scholarship No. 21110825, FONDECYT project No. 1151310 and No. 1130147.

## REFERENCES

- (1) Iqbal, M.; Gutsche, C. D. *Org. Synth.* **1993**, 8, 100–102.
- (2) Zhang, Wen-Chun; Huang, Z.-T. *Synthesis (Stuttg.)* **1997**, 9, 1073–1076.
- (3) Asfari, M.-Z.; Böhmer, V.; Harrowfield, J.; Vicens, J. *Calixarenes 2001*; Springer: Berlin, Germany, 2001.
- (4) Predeus, A. V.; Gopalsamuthiram, V.; Staples, R. J.; Wulff, W. D. *Angew. Chem. Int. Ed. Engl.* **2013**, 52 (3), 911–915.
- (5) Baldini, L.; Casnati, A.; Sansone, F. In *Comprehensive Supramolecular Chemistry II*; Atwood, J. L., Ed.; Elsevier: Oxford, 2017; pp 371–408.
- (6) Ukhatskaya, E. V.; Kurkov, S. V.; Matthews, S. E.; El Fagui, A.; Amiel, C.; Dalmas, F.; Loftsson, T. *Int. J. Pharm.* **2010**, 402 (1–2), 10–19.
- (7) Grives, S.; Phan, G.; Bouvier-Capely, C.; Suhard, D.; Rebiere, F.; Agarande, M.; Fattal, E. *Chem. Biol. Interact.* **2017**, 267, 33–39.
- (8) Zhao, B.; Liu, Y.; Zhang, H. *J. Mol. Struct.* **2004**, 691, 25–31.
- (9) Moris, S.; Galdámez, A.; Jara, P.; Saitz-barria, C. *Crystals* **2016**, 6 (114).
- (10) Perrin, M.; Ehlinger, N.; Lecocq, S.; Dumazet, I.; Lamartine, R. *J. Incl. Phenom. Macrocycl. Chem.* **2001**, 42 (82282), 273–276.
- (11) Mutihac, L.; Lee, J. H.; Kim, J. S.; Vicens, J. *J. Chem. Soc. Rev.* **2011**, 40 (5), 2777–2796.
- (12) M. Anthony McKervey, E. M. S. *J. Org. Chem.* **1986**, 51, 3581–3584.
- (13) Huang, G.; Jiang, L.; Wang, D.; Chen, J.; Li, Z.; Ma, S. *J. Mol. Liq.* **2016**, 220, 346–353.
- (14) C. Quiroga-Campano, H. Gomez-Machuca, S. Moris, P. Jara, J.R. de la Fuente, H. Pessoa-Mahana, C. Julian, C. S. *J. Mol. Struct.* **2017**, 1141, 133–141.
- (15) Collins, E.; Harriss, S. J.; Owens, M.; Ferguson, G.; Estate, I.; M. Anthony McKervey, E. M. S. *J. Chem. Soc. Perkin trans* **1991**, 3, 2–3.
- (16) Zhao, B.-T.; Liu, Y.; Zhang, H.-Y. *J. Mol. Struct.* **2004**, 691 (1–3), 25–31.
- (17) Rodriguez-Llamazares, S.; Jara, P.; Yutronic, N.; Noyong, M.; Bretschneider, J.; Simon, U. *J. Colloid Interface Sci.* **2007**, 316 (1), 202–205.
- (18) Li, H.; Yang, Y.-W. *Chinese Chem. Lett.* **2013**, 24 (7), 545–552.
- (19) Arduini, A.; Demuru, D.; Pochini, A.; Secchi, A. *Chem. Commun.* **2005**, No. 5, 645–647.
- (20) Sayin, S.; Ozcan, F.; Yilmaz, M. *Mater. Sci. Eng. C* **2013**, 33 (4), 2433–2439.
- (21) Dementjev, A. P.; Graaf, A. De; Sanden, M. C. M. Van De; Maslakov, K. I. *Diam. Relat. Mater.* **2000**, 9, 1904–1907.
- (22) Turkevich, J.; Stevenson, P. C.; Hillier, J. *Discuss. Faraday Soc.* **1951**, 11 (0), 55–75.
- (23) Lévy, R.; Thanh, N. T. K.; Doty, R. C.; Hussain, I.; Nichols, R. J.; Schiffrian, D. J.; Brust, M.; Fernig, D. G. *J. Am. Chem. Soc.* **2004**, 126 (32), 10076–10084.
- (24) Silva, N.; Moris, S.; Diaz, M.; Yutronic, N.; Lang, E.; Chornik, B.; Kogan, M. J.; Jara, P. *Molecules* **2016**, 21, 1–13.
- (25) Bruker SMART, SAINTPLUS V6.02, S. V. 1. and S. B. A. X. I. I.
- (26) Sheldrick, G.M. SHELLXL-97. Program for the Refinement of Crystal Structures; University of Göttingen: Stuttgart, G. 1997.
- (27) Pennington W. *J. Appl. Crystallogr.* **1999**, 32 (5), 1028–1029.
- (28) Speck, A. L. *J. Appl. Crystallogr.* **2003**, 36, 7–13.

- (29) Dieluweit, S.; Pum, D.; Sleytr, U. B.; Kautek, W. *Mat. Sci. Eng.* **2005**, *25*, 727–732.  
(30) Zhou, J. C.; Wang, X.; Xue, M.; Xu, Z.; Hamasaki, T.; Yang, Y.; Wang, K.; Dunn, B. *Mat. Sci. Eng. C* **2010**, *30* (1), 20–26.  
(31) Tseng, R. J.; Tsai, C.; Ma, L.; Ouyang, J.; Ozkan, C. S.; Yang, Y. *Nat. Nanotechnol.* **2006**, *1* (October), 4–9.  
(32) Kimura-suda, H.; Petrovykh, D. Y.; Tarlov, M. J.; Whitman, L. J. *J. Am. Chem.Soc* **2003**, *125*, 9014–9015.